

## CRYSTAL, MOLECULAR AND ELECTRONIC STRUCTURE OF METHYLTIN TRIIODIDE \*

J.S. TSE \*\*, M.J. COLLINS, F.L. LEE and E.J. GABE

*Division of Chemistry, National Research Council of Canada, Ottawa Ontario, K1A 0R9 (Canada)*

(Received November 12th, 1985)

### Summary

The crystal structure of methyltin triiodide ( $\text{CH}_3\text{SnI}_3$ ) has been determined by single crystal X-ray diffraction. It belongs to the orthorhombic space group  $Cmc2_1$ , with  $a$  10.3421(15),  $b$  13.1403(15) and  $c$  6.5700(8) Å. The  $\text{CH}_3\text{SnI}_3$  molecules are found to be discrete and loosely packed in the crystalline state. This observation is contrary to most methyltin halide structures in which the geometry at the tin atom is distorted from the ideal tetrahedron due to intermolecular coordination. The average Sn–I bond length of 2.6692(11) Å is shorter than those reported in similar compounds. Theoretical molecular orbital calculations show a small back-donation from the iodine atoms to the tin atom. The failure of the point charge model to predict the  $^{119}\text{Sn}$  Mössbauer quadrupole splitting of  $\text{CH}_3\text{SnI}_3$  is attributed to the partial double bond character of the Sn–I bonds.

---

### Introduction

Mössbauer spectroscopy is a very powerful technique to elucidate the electronic structure of tin compounds [1]. The chemical shift and quadrupole splitting contain valuable information on the mode of bonding and the local structure around the tin atom. Within a simple point charge approximation [2,3], the quadrupole splitting of the tin atom in a molecule can be decomposed into additive contributions from the constituent ligands. Therefore, the sign and magnitude of the quadrupole splitting are dependent on the nature of the ligands and their spatial arrangement [4,5]. Once a set of standard “partial quadrupole splittings” (pqs) values have been derived for different ligands from references compounds, it is then possible to deduce the local structure around the tin atom in an unknown compound from its quadrupole splittings. This approach has been very successful in distinguishing between *cis*- and

---

\* Published as NRCC 25382.

\*\* To whom correspondence should be addressed.

*trans*-R<sub>2</sub>SnL<sub>4</sub> isomers in the solid state [1]. Occasionally, deviation from the theoretical values can be accounted for by considering the distortion from the ideal geometry for four- and six-coordination [6].

One interesting prediction made by this simple model is that for four-coordinate organotin(IV) compounds, the magnitude of the quadrupole splitting of RSnL<sub>3</sub> should be the same but differ in sign from R<sub>3</sub>SnL [1]. So far, no such correlation has been observed in organotin halides [4,7–9]. In the case of the fluorides and chlorides, the discrepancy can be adequately resolved by noting the structural differences of the monohalide and trihalide in the solid state. The trihalide structures are usually polymeric with extensive bridging Sn–halide bonds [10–13]. As a result, the environment around the tin atom is strongly distorted from the regular tetrahedral geometry. The intermolecular interactions in the trialkyltin halides are much weaker and the distortions are not as significant. However, this explanation fails to rationalize the recent <sup>129</sup>I and <sup>119</sup>Sn Mössbauer studies of CH<sub>3</sub>SnI<sub>3</sub> and (CH<sub>3</sub>)<sub>3</sub>SnI [8,9]. The similarity of the results obtained from frozen solution (1.61 mm s<sup>-1</sup>) and solid state (1.68 mm s<sup>-1</sup>) studies strongly suggests that the molecules are probably non-associated in the crystalline state, yet the observed quadrupole splittings are at variance with the theoretical prediction. This observation casts serious doubt on the applicability of the additive model in the interpretation of quadrupole splittings in these compounds. Moreover, in view of the strong tendency of the methyltin halides in forming polymeric structures through bridging halide atoms in the solid state, it is important to determine the structure of CH<sub>3</sub>SnI<sub>3</sub> before a satisfactory explanation for the Mössbauer spectra can be sought. In this paper we have examined the crystal structure of the title compound using single-crystal X-ray diffraction. Theoretical *ab initio* and X $\alpha$ -SW calculations were made in order to understand the electronic structure of this compound.

## Experimental

### Preparation

CH<sub>3</sub>SnI<sub>3</sub> was prepared following the method of Jones et al. [9]. CH<sub>3</sub>SnCl<sub>3</sub> (Strem Chemicals Inc.) was reacted with a slight excess of sodium iodide in dry chloroform under nitrogen atmosphere for 4 h. The yellowish solution was filtered and the solvent evaporated under a stream of dry nitrogen. Bright yellow crystals were obtained by slow sublimation at 75°C of the solid in an evacuated sealed tube. The compound was characterized by its melting point and NMR spectrum [9].

### Crystal structure

A needle-shape crystal of dimension 0.04 × 0.12 × 0.24 mm was mounted inside a capillary. To avoid rapid decomposition, the crystal was coated with epoxy glue. Intensity data were measured using profile analysis with a Picker four-circle diffractometer with Mo-K $\alpha$  radiation. The data were corrected for absorption by Gaussian integration assuming  $\mu(\text{Mo-K}\alpha)$  to be 13.0 mm<sup>-1</sup>. Pertinent information regarding data collection, structure solution and refinement procedures are summarized in Table 1. Details of the computer programs used and experimental procedure can be found in ref. 14.

CH<sub>3</sub>SnI<sub>3</sub> crystallizes in the orthorhombic space group *Cmc*2<sub>1</sub> with *a* 10.3421(15), *b* 13.1403(15) and *c* 6.5700(8) Å. Positional and thermal parameters are given in

TABLE 1  
SUMMARY OF CRYSTAL DATA AND INTENSITY COLLECTION

Compound	CH <sub>3</sub> SnI <sub>3</sub>
Cryst. dims. (mm)	0.04 × 0.12 × 0.24
Space group	<i>Cmc</i> 2 <sub>1</sub> (No.36)
<i>a</i>	10.3421(15) Å
<i>b</i>	13.1403(15) Å
<i>c</i>	6.5700(8) Å
<i>Z</i>	4
Density, (g cm <sup>-3</sup> )	3.827 (calcd.)
Radiation	Mo-K <sub>α</sub> (λ 0.70930 Å)
μ (mm <sup>-1</sup> )	13.0
Scan	ω-2θ, θ <sub>max</sub> = 30°
Unique data with <i>F</i> <sub>0</sub> <sup>2</sup> > 2.5σ( <i>F</i> <sub>0</sub> <sup>2</sup> )	823
<i>R</i> <sub>w</sub>	0.019
<i>R</i> <sub>f</sub>	0.032
Max. residue e/Å <sup>3</sup>	0.95

TABLE 2  
POSITIONAL (Å) AND THERMAL PARAMETERS (×10<sup>3</sup> Å<sup>2</sup>) FOR CH<sub>3</sub>SnI<sub>3</sub> (with e.s.d.'s in parentheses)

Atom	<i>x</i>	<i>y</i>	<i>z</i>	<i>U</i> <sub>11</sub>	<i>U</i> <sub>22</sub>	<i>U</i> <sub>33</sub>	<i>U</i> <sub>12</sub>	<i>U</i> <sub>13</sub>	<i>U</i> <sub>23</sub>
Sn	1/2	0.29953(7)	0.19354	5.00(6)	4.68(5)	4.07(6)	0.00	0.00	0.29(6)
I(1)	1/2	0.10705(6)	0.32252(23)	7.79(7)	4.63(5)	8.31(9)	0.00	0.00	1.14(7)
I(2)	0.29469(7)	0.38859(4)	0.36390(19)	6.59(5)	8.01(5)	8.17(5)	2.14(4)	1.06(6)	-0.09(6)
C	1/2	0.3144(8)	-0.1299(21)	8.4(11)	5.7(7)	2.6(7)	0.00	0.00	0.8(9)

TABLE 3  
BOND DISTANCES (Å) AND ANGLES (°) (with e.s.d.'s in parentheses)<sup>a</sup>

Sn-I(1)	2.6675(12)
Sn-I(2)	2.6700(9)
Sn-C	2.134(14)
Sn...I(1)	5.8471(14)
Sn...I(2)	4.4822(13)
Sn...C	4.449(14)
C...I(1)	4.0322(12)
C...I(2)	3.9982(12)
I(1)-Sn-I(2)	106.40(3)
I(2)-Sn-I(2')	105.45(4)
I(1)-Sn-C	116.1(6)
I(2)-Sn-C	110.9(3)

<sup>a</sup> Primed atoms are related to their unprimed counterparts (*x, y, z*) by (*x,  $\bar{y}, z + \frac{1}{2}$* ).

Table 2. Bond distances and angles are in Table 3. A perspective drawing of the molecule in the crystal along with the labelling scheme is shown in Fig. 1. Tables of positional and thermal parameters, observed and calculated structure factors have been deposited as supplementary material.

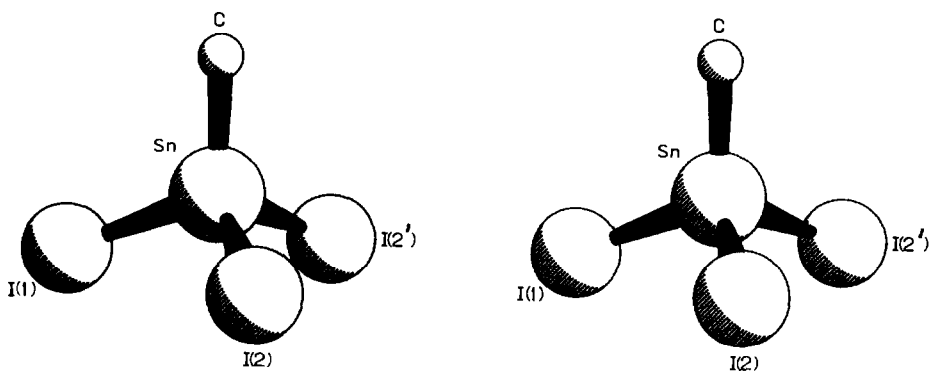


Fig. 1. A stereoview of the  $\text{CH}_3\text{SnI}_3$  molecule.

### Theoretical calculation

Ab initio molecular orbital calculations were performed on the experimental geometry with the average Sn–I bond length of 2.6692 Å. The effects of the core electrons are replaced with an appropriate effective potential (ECP). The full formalism for development and use of pseudopotential method have been documented extensively elsewhere [15,16]. In our calculations, the ECP for carbon atom was taken from the work of Stevens et al. [17], for Sn and I atom from the recent tabulation of Wadt and Hay [18]. The valence gaussian basis sets for the atoms were taken from ref. 17–19 and contracted to double zeta quality.

To complement the pseudopotential calculations which neglect the effect of inner valence Sn 4*d* orbitals to chemical bonding, we repeated the calculation employing the all electron quasi-relativistic X $\alpha$ -SW method [20–22]. The atomic exchange parameters  $\alpha_{\text{HF}}$  were taken from Schwarz [22]. The partial wave expansions were truncated at  $l_{\text{max}} = 4, 3, 3, 2,$  and 1 for the outer, tin, iodine, carbon and hydrogen spheres respectively.

### Results and discussion

The crystal structure of  $\text{CH}_3\text{SnI}_3$  is surprisingly simple. It consists of discrete monomeric molecules in almost ideal tetrahedral geometry. The  $\text{CH}_3\text{SnI}_3$  molecule uses a mirror plane at  $x = 0$  and  $1/2$  with I(1), Sn and C in the mirror plane and I(2) on either side. A stereoview of the  $\text{CH}_3\text{SnI}_3$  molecule is shown in Fig. 1. The  $\text{CH}_3\text{SnI}_3$  unit is very close to the ideal  $C_{3v}$  symmetry. The small structural distortion shows the lack of intermolecular coordination. The Sn–C bond of 2.134(14) Å is quite normal as compared with those in similar compounds. In the six-coordinated  $(\text{CH}_3)_2\text{SnF}_2$  [10] and  $(\text{CH}_3)_2\text{SnCl}_2$  [11] the Sn–C distances are 2.08(1) and 2.16(18) Å respectively. The average Sn–I distance of 2.6692(11) Å appears to be shorter than those observed in similar compounds. There are only a few tin–iodine bond lengths reported in the literature. In tin tetraiodide [23], diethyltin(IV) diiodide [13] and 1,4-bis(iododiphenyl)-1,4-distannabutane [24] the Sn–I bond lengths are 2.69(2), 2.719(4) and 2.729(3) Å respectively. Within the limits of the quoted standard deviations, the shorter Sn–I bond in  $\text{CH}_3\text{SnI}_3$  is statistically significant. The valence bonding angles deviate slightly from the regular

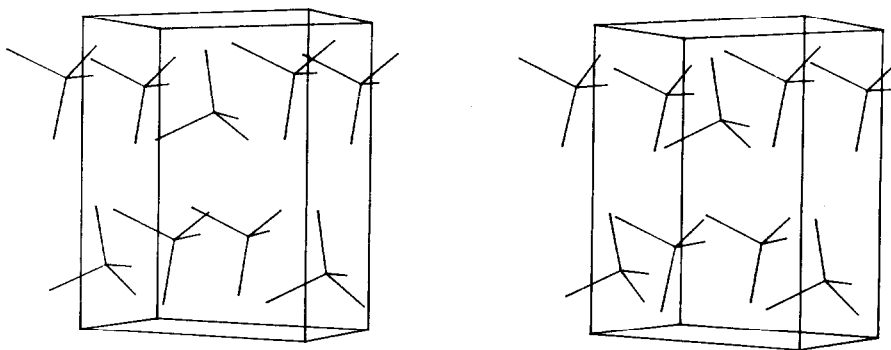


Fig. 2. Stereoscopic molecular packing diagram for  $\text{CH}_3\text{SnI}_3$ .

tetrahedral angles. The C–Sn–I(1) and C–Sn–I(2) angles are  $116.1(6)$  and  $110.9(3)^\circ$  while the I(1)–Sn–I(2) and I(2)–Sn–I(2') angles are  $106.40(3)$  and  $105.34(4)^\circ$  respectively. The larger C–Sn–I angles are consistent with the Bent's rule [25].

Since the methyl group is more electropositive than the iodine atoms, the electron pair in the Sn–C bond is more diffuse and closer to the central tin atom than are the electron pairs in the Sn–I bonds. Hence the Sn–C bond exerts the greatest repulsion.

The molecular packing diagram (Fig. 2) shows that the crystal is loosely packed and without any sign of significant intermolecular interaction. The closest Sn  $\cdots$  I intermolecular contact is between I<sub>2</sub> and the tin atom. The separation of  $4.4822(10)$  Å is longer than the sum of their Van der Waals radii ( $4.15$ – $4.32$  Å). In contrast, in diethyltin diiodide, the Sn  $\cdots$  I distance is  $4.285(5)$  Å. The shorter intermolecular distance reflects substantial secondary bonding between the atom with the neighbouring iodine atom. Furthermore, as a consequence of the nonbonded repulsion, the C–Sn–C bond angle was forced to open-up to  $130.20(11)^\circ$ . The small distortion in  $\text{CH}_3\text{SnI}_2$  is another good indication of the lack of intermolecular interaction. Surprisingly, the closest C  $\cdots$  I separation of  $3.998(12)$  Å in  $\text{CH}_3\text{SnI}_3$  is  $0.11$  Å shorter than the sum of their Van der Waals radii. This does not seem to affect the geometry of the  $\text{CH}_3\text{SnI}_3$  unit substantially. It also is interesting to observe that the methyl group of each  $\text{CH}_3\text{SnI}_3$  molecule is pointing into the base of the triad formed by the iodine atoms of the neighbouring molecule. However, the large Sn  $\cdots$  C distance of  $4.449(14)$  Å again precludes any possible intermolecular bonding. In view of the discreteness of the molecular packing, the electronic structure of  $\text{CH}_3\text{SnI}_3$  will not be significantly perturbed by the crystal environment. This explains the similarity of the Mössbauer results in the crystalline state and in frozen solution.

Discrete and non-coordinating organotin(IV) halides are seldom found in the solid state [26]. Intermolecular bonding through the halide atoms is common. The interaction is strongest for the fluorides and gets progressively weaker down the group. For instance, the dimethyltin difluoride is polymeric but the analogous dichloride compound is weakly coordinating. However, in some cases, mainly by experimental design, the intermolecular bonding can be eliminated by putting bulky groups onto the tin atoms. There have only been a few examples reported in the literature. Notable examples are the trialkyl- and triaryl-tin (IV) halides [26–28]. In

these compounds, the bulky R groups prohibit close Van der Waals contact between neighbouring molecules preventing the possibility of secondary bonding. To our knowledge, this is the first report of a monoalkyltin(IV) halide with discrete tetrahedral units in the crystalline state.

The  $^{119}\text{Sn}$  quadrupole splitting of  $1.68 \text{ mm s}^{-1}$  is much smaller than the predicted value of  $2.40 \text{ mm s}^{-1}$  from the partial quadrupole splittings of the iodides and methyl group assuming a tetrahedral arrangement of the ligands [1]. For similar tetrahedral organotin(IV) halides, the agreement with experiment is often better than a few percent. In most cases, the differences between observed and predicted values can be removed by considering the distortion of the molecule from the idealized geometry [27,29]. In the present case, no satisfactory agreement with experiment could be achieved by adjusting the C–Sn–I angle [6] within a reasonable range. It is surprising that the point charge model performed so poorly in this case. There are three possible reasons for the failure of the model. The assumption of a transferable pqs for a given ligand regardless of the nature of the other ligands in the compound may be too simplistic. Assuming the additive model is valid, we can calculate the pqs for the iodide ion in  $\text{CH}_3\text{SnI}_3$  from the observed quadrupole splitting. Using an accepted pqs value for methyl group of  $-1.37 \text{ mm s}^{-1}$ , the pqs value for iodine is found to be  $-0.53 \text{ mm s}^{-1}$ . The magnitude of the pqs seems quite large for the halogens which are usually very small and taken to be zero in most treatments [1]. The other alternative is that the sign of the QS may be reverse in this compound (see ref. 1b). Finally, the point charge approximation for the contribution to the field gradient of the tin nucleus from the iodine atoms may not be appropriate for this compound. To investigate this possibility, we have performed molecular orbital (MO) calculations in order to understand the electronic structure of  $\text{CH}_3\text{SnI}_3$ .

The salient features of the valence  $X\alpha$  molecular orbitals are given in Table 4. For each orbital, the electron density and their characters are tabulated. Similar charge distribution and MO ordering are also found with the ab initio calculation. The partition of electronic charge in the  $X\alpha$  method is obscured by the present of

TABLE 4

$X\alpha$  EIGENVALUES (Ryd) AND PERCENT CHARGE DISTRIBUTION FOR  $\text{CH}_3\text{SnI}_3$  <sup>a</sup>

Orbital	Energy	Outer	Inter	Sn	I	C	H
$1a_1$	-2.028	0.00	0.00	98.81(0.0)	0.05	0.01	0.00
$2a_1$	-1.393	0.00	15.06	16.64(6.1)	20.26	34.85	0.13
$3a_1$	-1.335	0.00	7.27	9.62(31.7)	62.26	14.34	6.23
$4a_1$	-0.965	0.01	2.83	52.55(0.0)	35.49	6.08	0.02
$5a_1$	-0.669	0.01	1.29	34.64(90.7)	22.47	25.81	3.60
$6a_1$	-0.529	1.61	20.87	4.28(7.0)	67.78	5.07	0.00
$1a_2$	-0.504	1.57	18.08	0.01(0.0)	79.53	0.00	0.00
$1e$	-2.028	0.00	0.00	98.36(0.0)	0.02	0.00	0.00
$2e$	-2.021	0.00	0.00	99.64(0.0)	0.00	0.00	0.00
$3e$	-1.305	0.00	2.58	5.65(65.6)	91.30	0.00	0.00
$4e$	-0.842	0.00	27.66	2.39(64.6)	0.81	39.09	30.00
$5e$	-0.662	2.06	1.32	28.89(89.9)	66.04	0.01	0.01
$6e$	-0.532	1.55	21.40	2.36(2.8)	74.68	0.00	0.00
$7e$	-0.515	1.54	19.40	1.56(0.0)	77.40	0.00	0.00

<sup>a</sup> Percentage Sn  $5p$  contribution is given in parentheses.

TABLE 5  
Ab initio VALENCE ORBITAL CHARGES FOR  $\text{CH}_3\text{SnI}_3$

Orbital	Sn	I	C	H
<i>s</i>	0.882	1.966	1.286	1.032
<i>p<sub>x</sub></i>	0.745	1.991	1.286	
<i>p<sub>y</sub></i>	0.745	1.327	0.942	
<i>p<sub>z</sub></i>	0.874	1.946	0.798	

intersphere region. It is more appropriate to analysis the charge distribution using the ab initio wave functions via Mulliken population analysis. The atomic orbital populations in  $\text{CH}_3\text{SnI}_3$  are reported in Table 5. The net charges on the Sn, I, C and H atoms are respectively  $+0.76e$ ,  $-0.23e$ ,  $+0.03e$  and  $-0.03e$ . The calculation suggests that the Sn–I bonds are fairly ionic with a charge disparity of almost one electronic charge. This result is in accordance with the high ionicity estimated from the Mössbauer chemical shift [8,9].

The valence molecular orbitals can be classified approximately into nonbonding Sn  $4d$  ( $1a_1$ ,  $1e$ ,  $2e$ ), I  $5s$  ( $3a_1$ ,  $3e$ ) and the I lone pairs ( $6a_1$ ,  $1a_2$ ,  $6e$ ,  $7e$ ); the bonding Sn–C ( $5a_1$ ), Sn–I ( $4a_1$ ,  $5e$ ) and the C–H ( $2a_1$ ,  $4e$ ). The wave functions of the relevant Sn–I bonding MOs are displayed in Figs. 3 and 4. The wave functions obtained from both ab initio and X $\alpha$ -SW calculations are consistent with each other. In the case of the fluorine lone pair  $5a_1$  orbital, the X $\alpha$  calculation underestimates the contribution from the Sn  $5p$  orbital but overemphasizes the antibonding Sn–C  $4d_{z^2}$  character. It is clear from the plots that the iodine atoms utilize their  $p$  orbitals in forming the bonds with the tin atom. The  $\sigma$  bonding framework is displayed in Figs. 3a and c (also Figs. 4a and c). However, in addition to the  $\sigma$  bonding, an appreciable degree of  $\pi$  bonding is also evident. This is vividly manifested in the  $5a_1$  molecular orbital where significant overlap is observed between the lone pair orbitals of the iodine atoms with the Sn  $5p$  orbital of the Sn–C bond. This interaction obviously is not the “ $d_{\pi}-p_{\pi}$ ” type interaction which one might invoke to explain  $\pi$ -bonding between Sn and I atoms [8,30–32]. The data presented in Table 4 show that the  $d$  character on the tin atom in these molecular orbitals is minimal. This kind of “back-donation” from the halides into the central atom perhaps seems quite unusual, such electronic effect have been invoked to explain the strengthening of C–F bonds in polyfluorinated saturated hydrocarbons [33]. A consequence of the  $\pi$  bonding is a redistribution of electron density from the iodines to the tin atom. This serves to lower the bond ionicity and helps to reduce the  $p$  electron imbalance on the tin atom. The ab initio Sn–I overlap population of 0.2245 indicates that the covalent interaction between the Sn and I atoms is significant. The enhanced covalency leads to a contraction of the Sn–I bond. The theoretical bonding picture evidently complies with the experimental observation on the shortening of the Sn–I bond. Since the iodine orbitals overlap with the Sn  $p_z$  lobe component extended from the Sn–C bond, the C–Sn–I valence angle will open-up to facilitate maximum interaction. This accounts for the slight distortion from the ideal tetrahedral angle.

In  $C_{3v}$  symmetry, the principal component of the electric field tensor is parallel to the symmetry axis ( $z$ ). The magnitude of the quadrupole splitting is governed by the

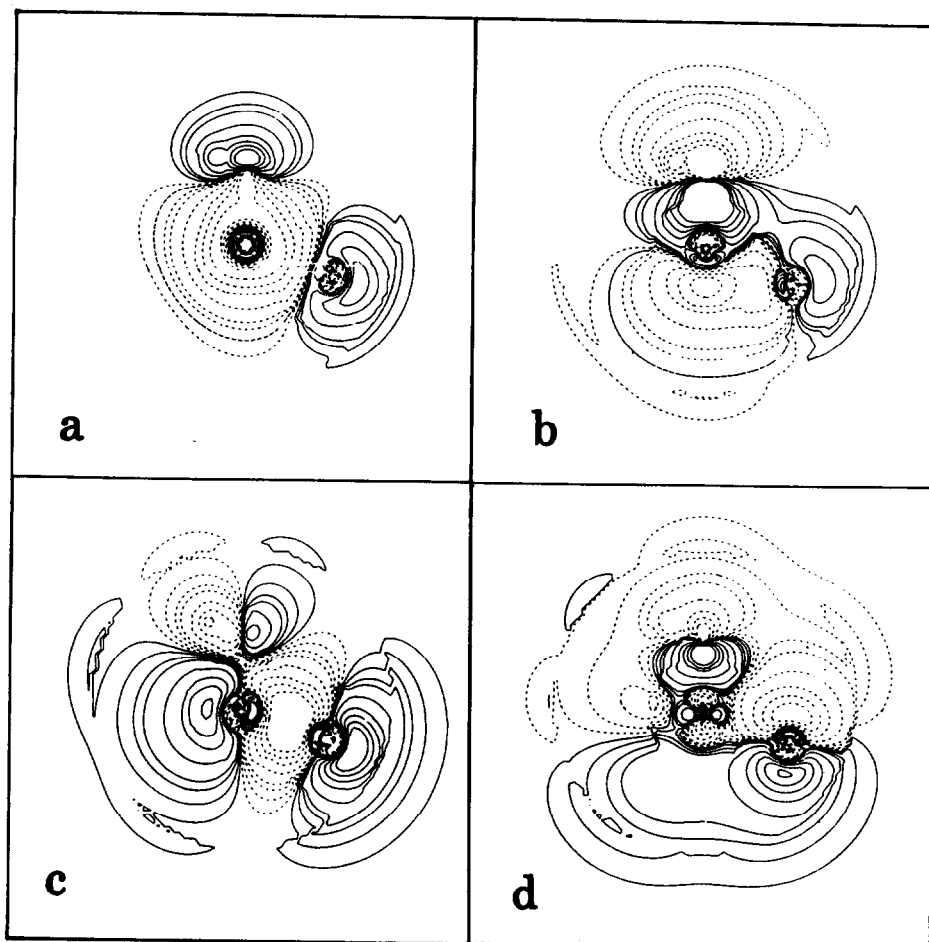


Fig. 3. Contour plots of the  $X\alpha$  wave functions for (a)  $3a_1$ ; (b)  $4a_1$ ; (c)  $5e$ ; and (d)  $5a_1$  molecular orbitals.

field gradient along this axis. It is proportional to the orbital charge imbalance in that direction. Knowing that the Sn  $p_z$  orbital transforms as  $a_1$  symmetry and the  $p_x$ ,  $p_y$  orbitals transform as  $e$  symmetry, we can calculate the charge imbalance from the charge density reported in Table 4 or 5 and using the following formula [34].

$$\Delta\rho = -N_{p_z} + 1/2(N_{p_x} + N_{p_y})$$

$\Delta\rho$  was found to be  $-0.09e$  by the  $X\alpha$  method and  $-0.13e$  by the *ab initio* calculation. In either case, the small charge imbalance clearly reflects the small observed quadrupole splitting. This is in direct contradiction with the value predicted by the additive model which emphasizes a concentration of charge along the axial Sn-C bond. The basic premise of the point charge model [2] and its MO variant [5] assumes  $\sigma$  bonding is the dominating electronic effect. No consideration of  $\pi$  bonding effects is possible within these models because the quadrupole

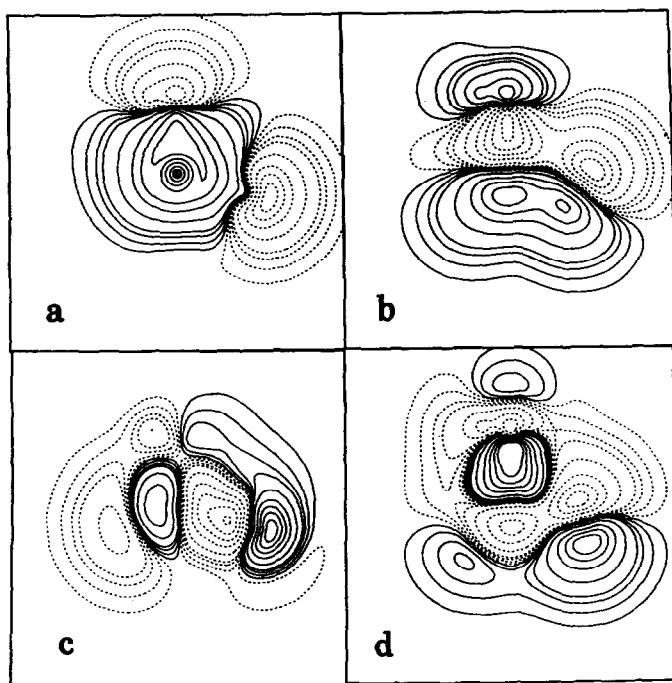


Fig. 4. Contour plots of the ab initio wave functions for (a)  $3a_1$ ; (b)  $4a_1$ ; (c)  $5e$ ; and (d)  $5a_1$  molecular orbitals.

splitting only depends on the spatial distribution of the ligands. These drastic assumptions have been proven to be reliable in most circumstances. However, in practice, derivation of the pqs value is often plagued by the lack of information on the detail geometry of the molecules. In order to achieve quantitative results, a different set of pqs values should be used for molecules with different coordination numbers.

### Concluding remarks

We found that crystalline  $\text{CH}_3\text{SnI}_3$  consists of non-coordinating discrete molecules. The short Sn–I bond length of 2.6692(13) Å reflects appreciable  $\pi$  bonding between the two atoms. Our result shows the previously derived pqs of iodine is not applicable in the  $\text{CH}_3\text{SnI}_3$  molecule. The additive model with the assumption of constant partial quadrupole splitting for a given ligand only applies to compounds with similar electronic and molecular structures. Our conclusion agrees with those of Drago et al. [8]. In addition, theoretical results show that failure of the point charge model lies in the neglect of the Sn–I  $\pi$  bonding effect. Therefore, the bonding in  $\text{CH}_3\text{SnI}_3$  cannot be interpreted adequately with simple  $\sigma$  Sn–I bonds. A correct description involves consideration of the partial double bond character.

### References

- 1 (a) G.M. Bancroft *Mössbauer Spectroscopy*, McGraw-Hill, London, 1972; (b) For a recent review see J.J. Zuckerman in R.H. Herber (Ed.), *Chemical Mössbauer Spectroscopy*, Plenum Press, New York, 1984.

- 2 R.V. Parish, *Prog. Inorg. Chem.*, 15 (1973) 101.
- 3 D. White and R.S. Drago, *J. Chem. Phys.*, 52 (1970) 4717.
- 4 G.M. Bancroft and R.H. Platt, in H.J. Emeléus and A.G. Shape (Eds.), *Advances Inorganic and Radiochemistry*, Academic Press, New York, 15 (1972) 59.
- 5 M.G. Clark, in A.D. Buckingham (Ed.), *MTP International Review of Science - Physical Chemistry*, Ser. 2, Butterworths, London, 1976.
- 6 T.K. Sham and G.M. Bancroft, *Inorg. Chem.*, 9 (1975) 2281
- 7 A.G. Maddock and R.H. Platt, *J. Chem. Soc., A* (1971) 1191.
- 8 A.P. Marks, R.S. Drago, R.H. Herber and M.J. Potasek, *Inorg. Chem.*, 15 (1976) 259.
- 9 C.H.W. Jones and M. Dombosky, *Canad. J. Chem.*, 59 (1981) 1585.
- 10 E.O. Schlemper and D. Briton, *Inorg. Chem.*, 5 (1966) 995.
- 11 A.G. Davis, H.J. Milledge, D.C. Puxley and P.J. Smith, *J. Chem. Soc., A* (1970) 2862.
- 12 P.T. Greene and R.F. Bryan, *J. Chem. Soc., A* (1971) 2549.
- 13 N.W. Alcock and J.F. Sawyer, *J. Chem. Soc., Dalton Trans.*, (1977) 1090.
- 14 (a) D.F. Grant and E.J. Gabe, *J. Appl. Cryst.*, 11 (1978) 114; (b) A.C. Larson and E.J. Gabe, in H. Schenk, R. Olthof-Hazekamp, H. van Koningsveld and G.C. Bassi (Eds.), *Computing in Crystallography*, Univ. Press, Delft 1978.
- 15 L.R. Kahn, P. Baybutt and D.G. Truhlar, *J. Chem. Phys.*, 65 (1976) 3826.
- 16 L.R. Kahn and W.A. Goddard III, *J. Chem. Phys.*, 56 (1972) 2685.
- 17 W.J. Stevens, H. Basch and M. Krauss, *J. Chem. Phys.*, 81 (1984) 6026.
- 18 W.R. Wadt and P.J. Hay, *J. Chem. Phys.*, 82 (1985) 284.
- 19 T.H. Dunning, *J. Chem. Phys.*, 53 (1970) 2823.
- 20 J.C. Slater, *The Calculation of Molecular Orbitals*, Wiley, New York, 1980.
- 21 K.H. Johnson, *Adv. Quant. Chem.*, 7 (1973) 143.
- 22 K. Schwarz, *Phys. Rev.*, B5 (1972) 2466.
- 23 F. Mellow and I. Fankuchen, *Acta Cryst.*, 8 (1955) 343.
- 24 V. Cody and E. Corey, *J. Organomet. Chem.*, 19 (1969) 359.
- 25 H.A. Bent, *Chem. Rev.*, 61 (1961) 275.
- 26 (a) J.A. Zubieta and J.J. Zuckerman, *Prog. Inorg. Chem.*, 24 (1978) 251 and reference therein; (b) P.J. Smith, *J. Organomet. Chem. Libr.*, 12 (1981) 97.
- 27 S. Calogero, P. Ganis, V. Peruzzo and G. Tagliavini, *J. Organomet. Chem.*, 179 (1979) 145.
- 28 S. Calogero, P. Ganis, V. Peruzzo, G. Tagliavini and G. Valle, *J. Organomet. Chem.*, 202 (1981) 22.
- 29 K. Molloy, K. Quill and I.W. Nowell, *J. Organomet. Chem.*, 289 (1985) 271.
- 30 T.C. Gibb and N.N. Greenwood, *J. Chem. Soc., A* (1967) 43.
- 31 N.N. Greenwood, P.G. Perkins and D.H. Wall, *Discuss. Faraday Soc.*, 1 (1968) 90.
- 32 J.J. Zuckerman, *Adv. Organomet. Chem.*, 9 (1971) 21.
- 33 L. Radom, W.J. Hehre and J.A. Pople, *J. Amer. Chem. Soc.*, 93 (1971) 289.
- 34 E.A.C. Lucken, *Nuclear Quadrupole Coupling Constants*, Academic Press, New York, 1967.